Journal of Renewable Materials

Tech Science Press

DOI: 10.32604/jrm.2021.011655

ARTICLE

Flexible Nanopaper Composed of Wood-Derived Nanofibrillated Cellulose and Graphene Building Blocks

Qing Li[1], Ming Dai[1], Xueren Qian[1], Tian Liu[1], Zhenbo Liu[1], Yu Liu[1], Ming Chen[1], Wang He[1], Suqing Zeng[1], Yu Meng[1], Chenchen Dai[1], Jing Shen[1], Yingtao Liu[1], Wenshuai Chen[1], Wenbo Liu[1,*] and Ping Lu[2,*]

[1]College of Material Science and Engineering, Northeast Forestry University, Harbin, 150040, China

[2]Department of Chemistry and Biochemistry, Rowan University, Glassboro, NJ, 08028, USA

[*]Corresponding Authors: Wenbo Liu. Email: hljlwbo@nefu.edu.cn; Ping Lu. Email: lup@rowan.edu

Received: 22 May 2020 Accepted: 11 August 2020

ABSTRACT

Nanopaper has attracted considerable interest in the fields of films and paper research. However, the challenge of integrating the many advantages of nanopaper still remains. Herein, we developed a facile strategy to fabricate multifunctional nanocomposite paper (NGCP) composed of wood-derived nanofibrillated cellulose (NFC) and graphene as building blocks. NFC suspension was consisted of long and entangled NFCs (10–30 nm in width) and their aggregates. Before NGCP formation, NFC was chemically modified with a silane coupling agent to ensure that it could interact strongly with graphene in NGCP. The resulting NGCP samples were flexible and could be bent repeatedly without any structural damage. Within the NGCP samples, the high aspect ratio of NFC made a major contribution to its high mechanical strength, whereas the sheet-like graphene endowed the NGCP with electrical resistance and electrochemical activity. The mechanical strength of the NGCP samples decreased as their graphene content increased. However, the electrical resistance and electrochemical activity of the NGCP samples both rose with increasing content of graphene. The NGCPs still kept advantageous mechanical properties even at high temperatures around 300°C because of the high thermal stability of NFCs and their strong entangled web-like structures. In view of its sustainable building blocks and multifunctional characteristics, the NGCP developed in this work is promising as low-cost and high-performance nanopaper.

KEYWORDS

Nanofibrillated cellulose; graphene; flexible nanopaper; mechanical strength; electrical resistance

1 Introduction

Cellulose is the most abundant renewable resource on Earth [1]. In recent years, the development of lignocellulosic substances as advanced functional materials has attracted considerable attention. Cellulose exists as nanofibers (microfibrils; elemental fibrils) within biomass resources such as wood [2], bamboo [3], and agricultural residues [4], and supports the bulk of higher plant fibers [5–8]. Cellulose nanofibers have multiple useful features including a nanoscale intrinsic structure; high aspect ratio; favorable surface chemistry because they contain numerous surface-active hydroxyl groups; strong mechanical performance, i.e., a high Young's modulus in the longitudinal direction of ~138 GPa [9] in their

crystalline regions and high specific strength; flexibility; high thermal stability; and a very low coefficient of thermal expansion (10^{-7} K^{-1}) [3]. Thus, many methodologies have been used to extract different types of nanocellulose from various biomass resources [10].

Nanofibrillated cellulose (NFC) is a specific kind of nanocellulose that has a high aspect ratio and web-like entangled networks [11]. NFC has been widely used to fabricate nanopaper [12,13]. Compared with ordinary paper composed of micrometer-sized cellulose pulp fibers, cellulose nanopaper has higher transparency, higher strength, and a lower coefficient of thermal expansion [14]. However, it remains desirable to introduce other novel functions—such as electrical conductivity and electrochemical activity—into nanopaper [15]. Nanocarbon has high electrical conductivity and satisfactory electrochemical properties [16]. Among the various forms of nanocarbon, graphene (GR) has become a research focus in materials science because of its excellent properties and unique two-dimensional (2D) lattice structure [17]. A 2D crystal of GR is composed of a single layer of sp^2 hybridized carbon atoms. Both GR and graphene oxide (GO) have been combined with other substances to prepare bulk materials with excellent performance including one-dimensional (1D) fibers, 2D paper, and three-dimensional (3D) hydrogels [18] and aerogels [19,20]. Such composite bulk materials have demonstrated considerable potential in many fields including energy storage [21], electronics, environmental purification, and catalysis [22,23].

The integration of 1D wood-derived NFC and 2D GR or GO can produce high-performance composite nanopaper [24,25]. In such nanopaper, the 1D NFC provides an entangled structure, active surface hydroxyl groups, and high mechanical strength, whereas the 2D GR or GO supplies electrical conductivity and electrochemical activity [26,27]. Nanopaper samples have been prepared by homogenously mixing an aqueous suspension of NFC with a dispersion of GR [28].The water in the reaction mixture was then largely removed by vacuum filtration. After hot-pressing or natural evaporation, NFC/GR composite nanopaper with excellent mechanical properties was produced [25]. Within composite nanopaper, a strong attractive interaction forms between GR and NFC. This interaction enhances the mechanical strength of the composite nanopaper and increases the synergistic effect of its building blocks [29,30]. Biomimetic composite nanopaper has been fabricated by integration of NFC and GR modified with proteins via genetic engineering [31]. Coating GR with protein facilitated its dispersion in the NFC matrix. We prepared nanopaper samples with high density and homogeneous structure at the microscale [14]. A lamellar alignment of the NFC and GR flakes was observed within the nanopaper, which led to satisfactory mechanical strength.

Although several methods to fabricate nanopaper using NFC and GR as building blocks have been developed, a simple, effective, and economical strategy for the large-scale production of nanopaper is still required. Moreover, an in-depth investigation of nanopaper and its components is necessary to improve the performance of nanopaper. Herein, we isolate NFC from wood by chemical pretreatment combined with high-pressure homogenization and nanofibrillation. The surface of the NFC is then modified using a silane coupling agent to promote the uniform dispersion of GR within the NFC suspension. The modified NFC and GR are integrated to produce multifunctional nanopaper (denoted as NGCP). The properties of NGCP, including flexibility, strength, electrical resistance, and electrochemical activity, are evaluated.

2 Experimental Section

2.1 Materials

NFC was isolated from poplar wood powder (60–80 mesh). The silane coupling agent (KH-570; ≥98%), single-layer GR powder (lamellar diameter: 0.5–2 μm; thickness: 0.8 nm; single layer rate: ~80%) was purchased from commercial resources, acetic acid, sodium chlorite ($NaClO_2$), potassium hydroxide (KOH), and hydrochloric acid (HCl) were all laboratory-grade chemicals that were used as received.

2.2 Preparation of NFC

The extraction of NFC was based on our previously reported method [14]. Wood powder was first treated with acidified $NaClO_2$ (75°C for 1 h; four times). Subsequently, the sample was treated with 2 wt% KOH at 90°C for 2 h. To obtain highly purified cellulose pulp, the sample was further treated with acidified $NaClO_2$ at 75°C for 1 h and then 5 wt% KOH at 90°C for 2 h. The sample was treated with HCl (0.3 mol/L) at 80°C for 2 h. After chemical pretreatment, an aqueous suspension of the purified cellulose pulp (0.2 wt%, 100 mL) was nanofibrillated for 20 min at 800 W using an ultrasonic generator (JY 99-IID, Ningbo Scientz Biotechnology Co., Ltd., China) equipped with cylindrical titanium alloy probe tip (diameter: 15 mm). The slurry was treated with a homogenizer (APV-2000, SPW, Charlotte, NC, USA) for 20 min to produce an aqueous suspension of NFC. In the homogenizer, homogenizing valve 1 was operated at a pressure of 80–100 bar (8–10 MPa) and homogenizing valve 2 was operated at 350–450 bar (35–45 MPa).

2.3 Preparation of Silane Coupling Agent-Modified NFC

KH570 (5 g), methanol (18 g), and distilled water (2 g) were stirred together for 10 min. The pH of the solution was then adjusted to 3.5–4 using acetic acid. The solution was added to the aqueous suspension of NFC (0.2 wt%, 100 mL). The mixture was agitated for 2 h at 45°C to produce the silane coupling agent-modified NFC.

2.4 Preparation of GR Aqueous Suspension

GR (0.05 g) was added to distilled water (24.95 g) and dispersed in an ultrasonic cleaner for 40 min. Polyvinylpyrrolidone (PVP) (0.25 g) was added to the GR suspension. The mixture was agitated by an ultrasonic cleaner for 40 min to provide the GR aqueous suspension.

2.5 Preparation of NGCP

The GR suspension was added to the modified NFC aqueous suspension. The mixture was stirred at 45°C for 2–3 h and then cooled to room temperature. An aliquot of the suspension (10 mL) was vacuum filtered. The obtained wet sheet was placed on a silicon wafer and then dried at room temperature for 2–3 days to produce the NGCP.

2.6 Characterization

Transmission electron microscopy (TEM; Tecnai G2, FEI, USA) was conducted to investigate the morphology of NFC and GR. The NGCP samples were also imaged by scanning electron microscopy (SEM; Quanta 200, FEI, USA). Fourier-transform infrared (FTIR) spectroscopy (Magna 560 Nicolet, Thermo Electron, USA) was performed in the range of 400–4000 cm^{-1} at a resolution of 4 cm^{-1}. The mechanical properties of NGCP were determined using a universal mechanical testing machine (TA120-6AA, Zhonghang Electronic Measuring Instruments Co., Ltd., China) at a tensile speed of 1 mm/min at room temperature. An RST-8 four-probe tester (Guangzhou four probe technology., Guangzhou, China) was used to measure the resistance of the NGCP samples. Electrochemical measurements of NGCP were performed in a three-electrode system in which platinum foil and Hg/HgO electrodes were used as counter and reference electrodes, respectively. Aqueous KOH solution (3 mol/L) was used as the electrolyte. All potential difference values were normalized to the same reference electrode. The electrochemical measurements were carried out on a CHI660D electrochemical workstation (Chenhua Instrument Co., Shanghai, China).

The specific capacitance of the electrode was calculated according to the following equation:

$$C = 2S/(\Delta V m \gamma) \tag{1}$$

where C is the specific capacitance (F/g), S is the integral area obtained from the cyclic voltammetry measurements, ΔV is the potential window, m is the quantity of the sample (g), and γ is the scan rate (mV/s).

3 Results and Discussion

3.1 Fabrication of NGCPs

The preparation of the NGCP samples is represented schematically in Fig. 1. A trace amount of the silane coupling agent (KH570) was added to an NFC aqueous suspension to ensure the homogeneous dispersion of the high-aspect-ratio wood-derived NFC in water. KH570 reacted with the hydroxyl groups to form silane groups on the NFC surface, thereby suppressing aggregation and ensuring uniform dispersion of NFC in water. A GR aqueous dispersion was then added to the NFC suspension, followed by gentle stirring. A thin and uniform NGCP was obtained after vacuum filtration and drying the wet sheet at room temperature. The contents of the building blocks in the NGCP can be easily controlled by adjusting the volumes of the NFC and GR suspensions mixed together. The resulting NGCP samples are referred to as NGCP-x, where x is the weight percentage of GR in the NGCP.

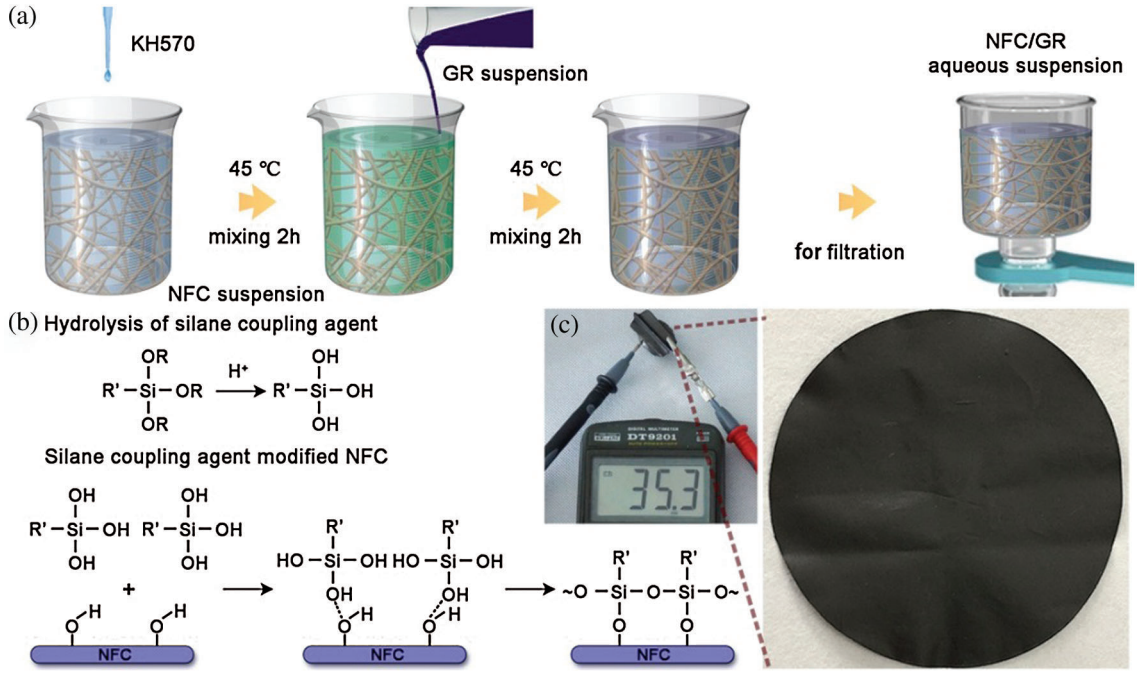

Figure 1: (a) Schematic diagram showing the fabrication of the NGCP. (b) Synthesis of KH570-modified wood-derived NFC. (c) Digital photographs showing an NGCP sample and its resistance

3.2 Characteristics of NGCP

As shown in the TEM images in Fig. 2, when NFC and GR were homogeneously mixed, the flake-like GR became interconnected with the high-aspect-ratio NFC network to form NGCP. The as-obtained NGCP was flexible and tailorable. Cross-sectional SEM images of NGCP samples are shown in Fig. 3. The NGCP samples had layered structures that were similar to that of nacre. The thickness of the NGCP sample increased with the GR content. The sheet-like GR and fiber-like NFC were closely interconnected within the NGCP and there were no obvious defects. Energy-dispersive X-ray spectroscopy (EDS) analyses of NGCO samples revealed that they were mainly composed of carbon (C) and oxygen (O) (Figs. 3d, 3h and 3l). A trace amount of silicon (Si) was also present, which originated from the silane coupling agent.

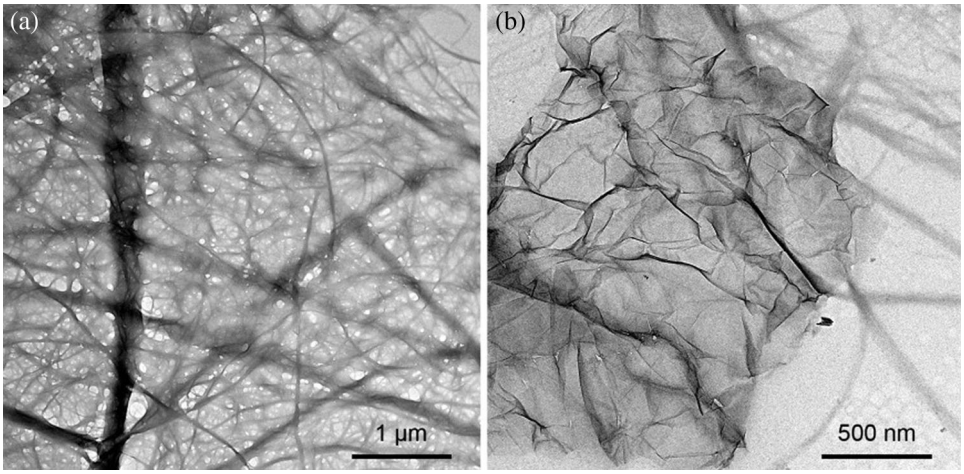

Figure 2: (a) Transmission electron microscopy (TEM) image of wood-derived NFC. (b) TEM image of NFC and graphene (GR) obtained from an NFC/GR mixture

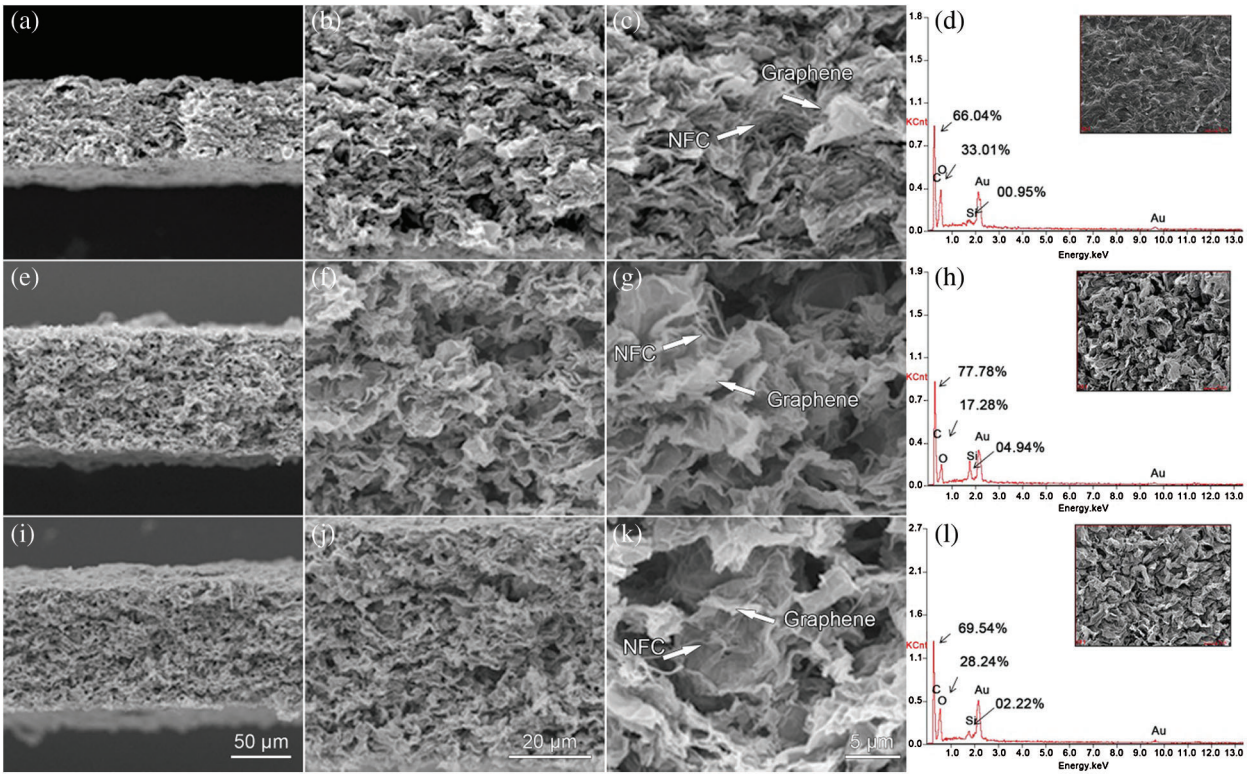

Figure 3: Scanning electron microscopy images of (a–c) NGCP-10, (e–g) NGCP-45, and (h–j) NGCP-70. Energy-dispersive X-ray spectra measured from the surfaces of (d) NGCP-10, (h) NGCP-45, and (l) NGCP-70, as shown in the corresponding insets

FTIR spectra of NFC and NGCP samples are shown in Fig. 4. The dominant peaks ascribed to O–H stretching and C–H stretching were located at approximately 3406 and 2900 cm^{-1}, respectively. The peaks at 1100 and 897 cm^{-1} were attributed to the C–O stretching and C–H deformation vibrations of cellulose,

respectively. There were no observable differences between the FTIR spectra of NFC and the NGCP samples, suggesting that the introduction of GR did not change the molecular structure of NFC in NGCP.

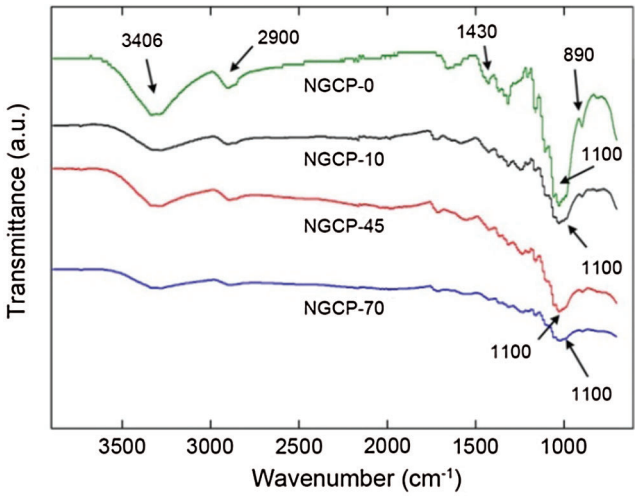

Figure 4: Fourier-transform infrared spectra of nanofibrillated cellulose (labeled as NGCP-0) and NGCP samples with different graphene contents

Because the NFC and GR were closely interconnected in the NGCP samples, they possessed high mechanical strength and flexibility. As shown in Fig. 5a, the NGCP samples were able to be bent and folded repeatedly without any noticeable damage. Moreover, the surfaces of the NGCP samples were smooth (Fig. 5b). Complete stress–strain curves of NGCP samples with various GR contents are shown in Fig. 5c. NGCP-10 had the greatest mechanical strength of the samples, with a tensile stress of approximately 55 MPa. The mechanical strength of the NGCP samples decreased with increasing GR content. The tensile stress of NGCP-70 was approximately 0.5 MPa. The Young's moduli of the NGCPs (Fig. 5e) followed a similar trend to that of their mechanical strength. The Young's modulus of NGCP-10 was 29 MPa, whereas that of NGCP-70 was only 2 MPa. Therefore, NFC played a critical role in enhancing the mechanical properties of NGCP.

Fig. 6a illustrates the conduction mechanism of NGCP. The surface of NFC possesses numerous hydroxyl groups, which were activated by the silane coupling agent. In NGCP, NFC and GR were closely interconnected through intermolecular forces such as hydrogen bonding and van der Waals interactions. The conductive GR and insulating NFC were entangled to form continuous conductive pathways, which endowed the composite with good electrical resistance. The electrical resistance of the NGCP samples was high when their GR content was low. The resistance of NGCP-10 was 200–350 kΩ. When the GR content increased to 70 wt% (i.e., in NGCP-70), the resistance decreased to 0.4–1.0 kΩ (Fig. 6b). These results illustrated that the resistance of the NGCPs decreased and their electrical performance increased as the GR content increased. A four-probe tester was used to further evaluate the electrical properties of the composite paper (Fig. 6c). The resistance of NGCP-10 was 280–550 kΩ, whereas that of NGCP-70 was only 0.1–0.5 kΩ. Therefore, the introduction of GR significantly improved the electrical performance of NGCP. The electrochemical properties of the NGCPs were investigated by cyclic voltammetry (see Figs S1–S3 in the Supporting Information). The cyclic voltammetry curves of the NGCPs with various NFC/GR ratios were closed, indicating high stability, and their areas increased with GR content, indicating that a higher GR content resulted in better electrochemical properties. As the sweep rate increased, the areas of the cyclic voltammetry curves of the NGCP samples increased and their specific capacitance decreased. The specific capacitance of the NGCP samples increased with their GR content up to 24 F/g

for NGCP-70. The addition of GR improved the electrochemical properties of NGCPs, but their performance was still lower than those of other graphene composites (see Fig. S4 in the Supporting Information).

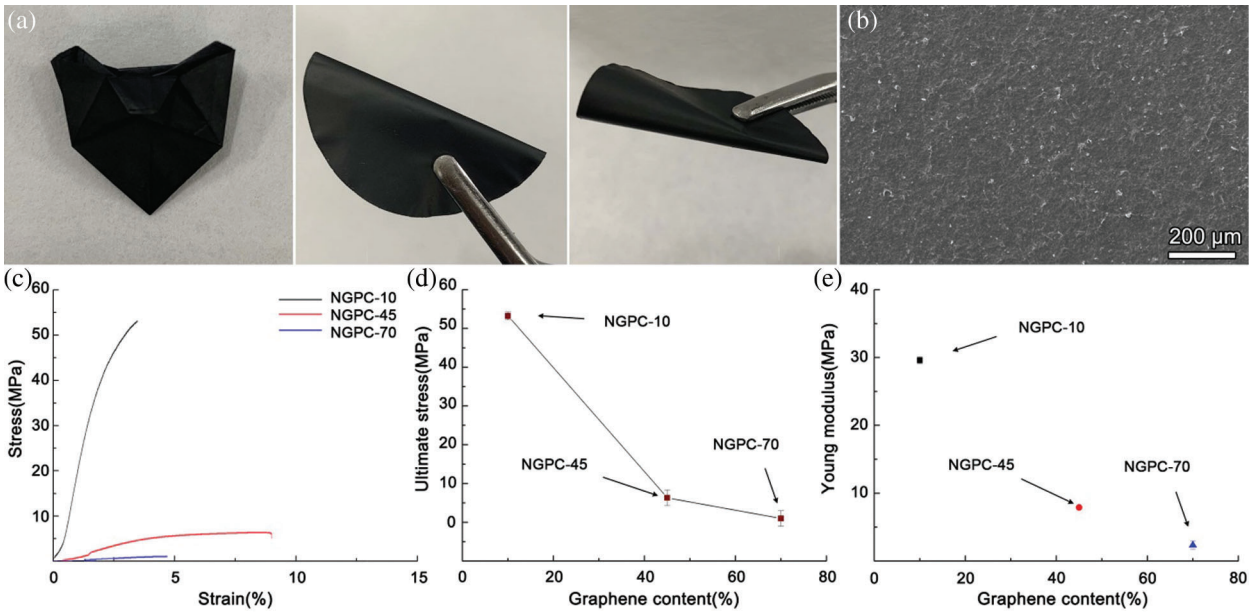

Figure 5: (a) Digital photographs of NGCP-10. (b) Scanning electron microscopy image of surfaces of NGCP-10. (c) Stress–Strain curves, (d) Ultimate tensile stress values, and (e) Young's moduli of NGCP samples with different graphene contents

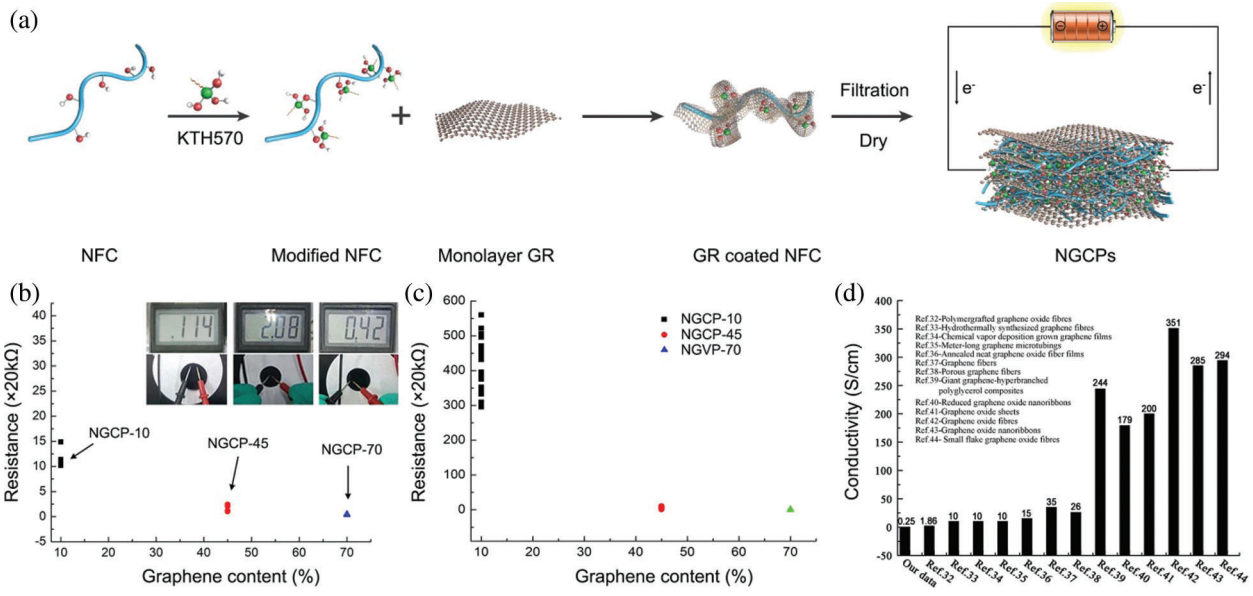

Figure 6: (a) Conduction mechanism of the NGCP. Resistance of the NGCP samples determined by (b) a multimeter and (c) the four-point probe method. (d) Conductivity of the NGCP samples compared with different materials

4 Conclusions

We fabricated NGCP using wood NFC and GR as building blocks. The silane coupling agent-modified NFC and GR were closely interconnected within the NCGP samples. The NGCP samples were flexible and could be bent and folded repeatedly without any observable damage. NGCP-10 had a tensile strength of approximately 55 MPa and Young's modulus of 29 MPa. The mechanical strength of the NGCP samples decreased as their GR content increased. However, the electrical resistance of the NGCP samples was raised by the introduction of GR. The electrical resistance of NGCP-70 was 0.1–0.5 kΩ. Because of the electrochemical activity of GR, the NGCP samples also exhibited favorable electrochemical performance. The specific capacitance of the NGCP samples increased with their GR content.

Acknowledgement: We acknowledge Xianhui An, Yuanyuan Miao, and others from the Northeast Forestry University for assisting with tests. We thank Natasha Lundin, PhD, from Liwen Bianji, Edanz Editing China (www.liwenbianji.cn/ac), for editing the English text of a draft of this manuscript.

Funding Statement: This research was funded by the National Natural Science Foundation of China (Grant No. 31800487), the Natural Science Foundation of Heilongjiang Province of China (Grant No. QC2018018), the Fundamental Research Funds for the Central Universities (Grant No. 2572019BB03), and the Foundation of Key Laboratory of Pulp and Paper Science and Technology of Ministry of Education/Shandong Province of China (Grant No. KF201721). Any research results expressed in this paper are those of the writer(s) and do not necessarily reflect the views of the foundations.

Conflicts of Interest: The authors declare that they have no conflicts of interest to report regarding the present study.

References

1. Abe, K., Iwamoto, S., Yano, H. (2007). Obtaining cellulose nanofibers with a uniform width of 15 nm from wood. *Biomacromolecules, 8(10),* 3276–3278. DOI 10.1021/bm700624p.
2. Uetani, K., Yano, H. (2010). Nanofibrillation of wood pulp using a high-speed blender. *Biomacromolecules, 12(2),* 348–353. DOI 10.1021/bm101103p.
3. Abe, K., Yano, H. (2010). Comparison of the characteristics of cellulose microfibril aggregates isolated from fiber and parenchyma cells of Moso bamboo (*Phyllostachys pubescens*). *Cellulose, 17(2),* 271–277. DOI 10.1007/s10570-009-9382-1.
4. Abe, K., Yano, H. (2009). Comparison of the characteristics of cellulose microfibril aggregates of wood, rice straw and potato tuber. *Cellulose, 16(6),* 1017–1023. DOI 10.1007/s10570-009-9334-9.
5. Chen, W., Li, Q., Wang, Y., Yi, X., Zeng, J. et al. (2014). Comparative study of aerogels obtained from differently prepared nanocellulose fibers. *ChemSusChem, 7(1),* 154–161. DOI 10.1002/cssc.201300950.
6. Chen, W., Yu, H., Lee, S. Y., Wei, T., Li, J. et al. (2018). Nanocellulose: A promising nanomaterial for advanced electrochemical energy storage. *Chemical Society Reviews, 47(8),* 2837–2872. DOI 10.1039/C7CS00790F.
7. Chen, W., Yu, H., Liu, Y., Chen, P., Zhang, M. et al. (2011). Individualization of cellulose nanofibers from wood using high-intensity ultrasonication combined with chemical pretreatments. *Carbohydrate Polymers, 83(4),* 1804–1811. DOI 10.1016/j.carbpol.2010.10.040.
8. Chen, W., Yu, H., Liu, Y., Hai, Y., Zhang, M. et al. (2011). Isolation and characterization of cellulose nanofibers from four plant cellulose fibers using a chemical-ultrasonic process. *Cellulose, 18(2),* 433–442. DOI 10.1007/s10570-011-9497-z.
9. Sakurada, I., Nukushina, Y., Ito, T. (1962). Experimental determination of the elastic modulus of crystalline regions in oriented polymers. *Journal of Polymer Science, 57(165),* 651–660. DOI 10.1002/pol.1962.1205716551.
10. Habibi, Y. (2014). Key advances in the chemical modification of nanocelluloses. *Chemical Society Reviews, 43(5),* 1519–1542. DOI 10.1039/C3CS60204D.

11. Li, Y., Liu, Y., Chen, W., Wang, Q., Liu, Y. et al. (2016). Facile extraction of cellulose nanocrystals from wood using ethanol and peroxide solvothermal pretreatment followed by ultrasonic nanofibrillation. *Green Chemistry, 18(4),* 1010–1018. DOI 10.1039/C5GC02576A.
12. Nishino, T., Takano, K., Nakamae, K. (1995). Elastic modulus of the crystalline regions of cellulose polymorphs. *Journal of Polymer Science Part B: Polymer Physics, 33(11),* 1647–1651. DOI 10.1002/polb.1995.090331110.
13. Nogi, M., Iwamoto, S., Nakagaito, A. N., Yano, H. (2009). Optically transparent nanofiber paper. *Advanced Materials, 21(16),* 1595–1598. DOI 10.1002/adma.200803174.
14. Li, Q., Chen, W., Li, Y., Guo, X., Song, S. et al. (2016). Comparative study of the structure, mechanical and thermomechanical properties of cellulose nanopapers with different thickness. *Cellulose, 23(2),* 1375–1382. DOI 10.1007/s10570-016-0857-6.
15. Shirakawa, H., Louis, E. J., MacDiarmid, A. G., Chiang, C. K., Heeger, A. J. (1977). Synthesis of electrically conducting organic polymers: Halogen derivatives of polyacetylene, (CH)x. *Journal of the Chemical Society, Chemical Communications, 16,* 578–580. DOI 10.1039/c39770000578.
16. Lee, C., Wei, X., Kysar, J. W., Hone, J. (2008). Measurement of the elastic properties and intrinsic strength of monolayer graphene. *Science, 321(5887),* 385–388. DOI 10.1126/science.1157996.
17. Du, X., Skachko, I., Barker, A., Andrei, E. Y. (2008). Approaching ballistic transport in suspended graphene. *Nature Nanotechnology, 3(8),* 491–495. DOI 10.1038/nnano.2008.199.
18. Huang, H., Zeng, X., Li, W., Wang, H., Wang, Q. et al. (2014). Reinforced conducting hydrogels prepared from the *in situ* polymerization of aniline in an aqueous solution of sodium alginate. *Journal of Materials Chemistry A, 2(39),* 16516–16522. DOI 10.1039/C4TA03332A.
19. Bae, S. Y., Jeon, I. Y., Yang, J., Park, N., Shin, H. S. et al. (2011). Large-area graphene films by simple solution casting of edge-selectively functionalized graphite. *ACS Nano, 5(6),* 4974–4980. DOI 10.1021/nn201072m.
20. Wang, Z., Shen, X., Akbari Garakani, M., Lin, X., Wu, Y. et al. (2015). Graphene aerogel/epoxy composites with exceptional anisotropic structure and properties. *ACS Applied Materials & Interfaces, 7(9),* 5538–5549. DOI 10.1021/acsami.5b00146.
21. Hu, H., Zhao, Z., Wan, W., Gogotsi, Y., Qiu, J. (2014). Polymer/graphene hybrid aerogel with high compressibility, conductivity, and "sticky" superhydrophobicity. *ACS Applied Materials & Interfaces, 6(5),* 3242–3249. DOI 10.1021/am4050647.
22. Chen, L., He, Y., Chai, S., Qiang, H., Chen, F. et al. (2013). Toward high performance graphene fibers. *Nanoscale, 5(13),* 5809–5815. DOI 10.1039/c3nr01083j.
23. Fang, B., Peng, L., Xu, Z., Gao, C. (2015). Wet-spinning of continuous montmorillonite-graphene fibers for fire-resistant lightweight conductors. *ACS Nano, 9(5),* 5214–5222. DOI 10.1021/acsnano.5b00616.
24. Lai, F., Franceschini, I., Corrias, F., Sala, M. C., Cilurzo, F. et al. (2015). Maltodextrin fast dissolving films for quercetin nanocrystal delivery. A feasibility study. *Carbohydrate Polymers, 121,* 217–223. DOI 10.1016/j.carbpol.2014.11.070.
25. Liu, Y., Zhou, J., Zhu, E., Tang, J., Liu, X. et al. (2015). Facile synthesis of bacterial cellulose fibres covalently intercalated with graphene oxide by one-step cross-linking for robust supercapacitors. *Journal of Materials Chemistry C, 3(5),* 1011–1017. DOI 10.1039/C4TC01822B.
26. Wang, Z., Tammela, P., Strømme, M., Nyholm, L. (2015). Nanocellulose coupled flexible polypyrrole@graphene oxide composite paper electrodes with high volumetric capacitance. *Nanoscale, 7(8),* 3418–3423. DOI 10.1039/C4NR07251K.
27. Gao, K., Shao, Z., Li, J., Wang, X., Peng, X. et al. (2013). Cellulose nanofiber–graphene all solid-state flexible supercapacitors. *Journal of Materials Chemistry A, 1(1),* 63–67. DOI 10.1039/C2TA00386D.
28. Li, Z., Liu, J., Jiang, K., Thundat, T. (2016). Carbonized nanocellulose sustainably boosts the performance of activated carbon in ionic liquid supercapacitors. *Nano Energy, 25,* 161–169. DOI 10.1016/j.nanoen.2016.04.036.
29. Li, Y., Zhu, H., Li, Y., Zhu, H., Shen, F. et al. (2014). Highly conductive microfiber of graphene oxide templated carbonization of nanofibrillated cellulose. *Advanced Functional Materials, 24(46),* 7366–7372. DOI 10.1002/adfm.201402129.

30. Wang, B., Li, X., Luo, B., Yang, J., Wang, X. et al. (2013). Pyrolyzed bacterial cellulose: A versatile support for lithium ion battery anode materials. *Small, 9(14),* 2399–2404. DOI 10.1002/smll.201300692.
31. Patel, A. R., Heussen, P. C., Hazekamp, J., Drost, E., Velikov, K. P. (2012). Quercetin loaded biopolymeric colloidal particles prepared by simultaneous precipitation of quercetin with hydrophobic protein in aqueous medium. *Food Chemistry, 133(2),* 423–429. DOI 10.1016/j.foodchem.2012.01.054.

Supplemental Figures

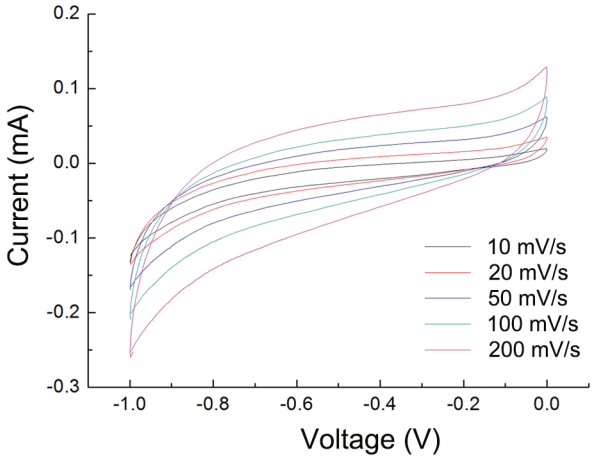

Figure S1: Cyclic voltammograms of NGCP-10

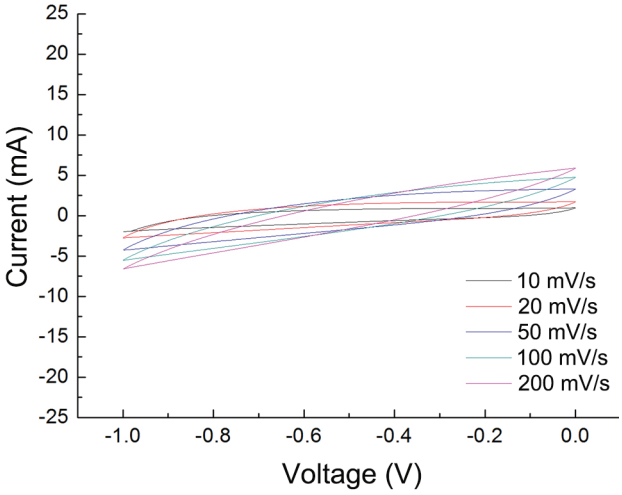

Figure S2: Cyclic voltammograms of NGCP-45

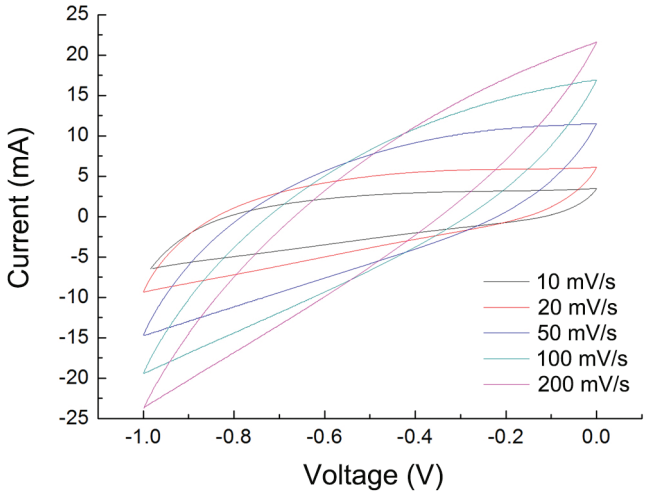

Figure S3: Cyclic voltammograms of NGCP-70

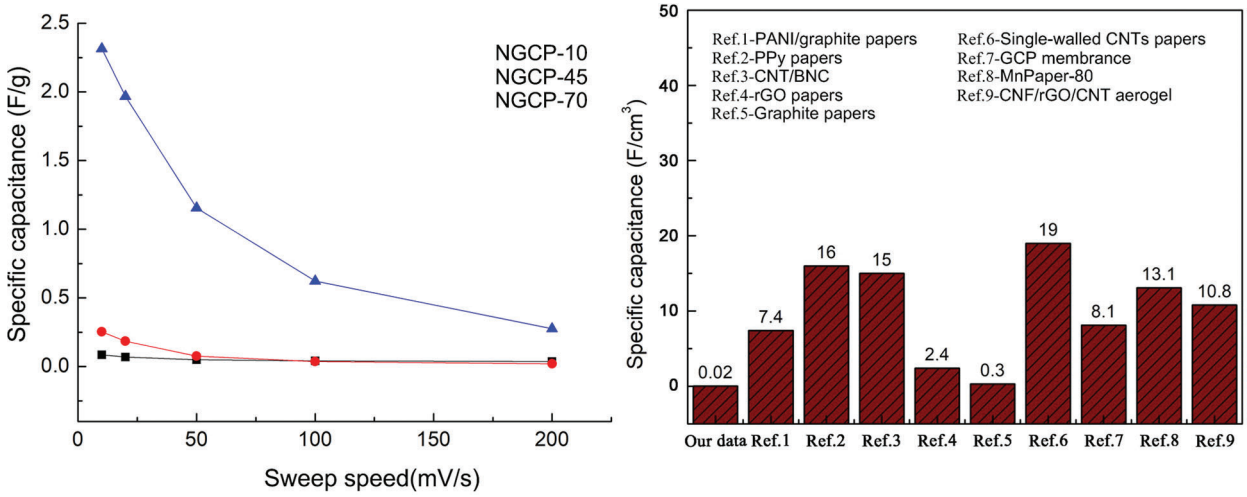

Figure S4: Electrochemical properties of NGCPs (left) compared with different materials (right)